Wireless Networks (2021) 27:4967–4985
https://doi.org/10.1007/s11276-021-02770-4

ORIGINAL PAPER

C-shaped antenna based artificial magnetic conductor structure for wearable IoT healthcare devices

Adel Y. I. Ashyap[1] · S. H. Dahlan[1] · Z. Z. Abidin[2] · M. R. Kamarudin[2] · H. A. Majid[1] · Nayef Abdulwahab Mohammed Alduais[3] · M. Hashim Dahri[4] · Somya Abdulkarim Alhandi[3]

Accepted: 25 August 2021 / Published online: 12 September 2021

Abstract

A wearable C-shaped antenna based on a fabric material operating at 2.4 GHz frequency is proposed for use in flexible/wearable IoT medical systems. The wearable IoT device plays a key role in medical applications, and the antenna is a key part of it. Loading the presented antenna on the body models showed a frequency detuned with the gain and efficiency reduced from 1. 28 to −9 dB and 90% to 10%. In addition, the SAR did not meet the safety health requirement defined by the FCC or ICNIRP standards. Therefore, an "Artificial Magnetic Conductor" structure (AMC) is added to the C-shaped antenna to overcome these problems. The AMC acts as shielding material between the human skin and the presented antenna because of its 0° reflection phase, which mimics the action of the Perfect Magnetic Conductor (PMC). The overall size of the proposed design was 54 × 54 × 3.9 mm^3. Numerical and experimental findings indicated that integrating the AMC structures with a C-shaped antenna was robust for body deformation and load. The C-shaped antenna worked equally well with the AMC, whether positioned in free space or on the chest or the arm of the human body. The integrated antenna with AMC structures has excellent performances. The gain and efficiency without loading on the chest were 6.49 dB and 84%, respectively. While for loaded on the chest were 6.21 dB and 81%, respectively. It also decreased the back radiation and raised the Front to Back Ration (FBR) by 13.8 dB. SAR levels have been reduced by more than 90% between the FCC and ICNIRP standards compared to the C-shaped antenna alone, which does not comply with the standards. As a result, the C-shaped integration with AMC structures is highly suitable for assembly in any wearable system.

Keywords Wearable · Specific absorption rate (SAR) · Healthcare · ISM-band

1 Introduction

The Internet of Things (IoT) has recently brought new challenges to researchers. It shifts the idea of interaction between people and the environment. In addition, it is considered to be one of the most innovative emerging technologies to support interactions between objects, as shown in Fig. 1. It is predicted that human life can be made more comfortable, stable, secure, and efficient by addressing several difficulties related to logistics, manufacturing, urbanization, energy, and the environment. Its device can transfer data to users or users to a computer interaction without interaction. [1, 2].

Wearable IoT systems are one of the significant roles in medical applications, for example temperature control and sensing, heart-rate, and wellness information [4, 5]. Figure 2 demonstrates the architecture of the IoT-based health monitoring system. Various components that were

✉ S. H. Dahlan
samsulh@uthm.edu.my

✉ Z. Z. Abidin
zuhairia@uthm.edu.my

[1] Faculty of Electrical and Electronic Engineering, Center for Applied Electromagnetic (EM Center), Universiti Tun Hussein Onn Malaysia, (UTHM), 86400 Batu Pahat, Johor, Malaysia

[2] Faculty of Electrical and Electronic Engineering, Advanced Telecommunication Research Center (ATRC), Universiti Tun Hussein Onn Malaysia, (UTHM), 86400 Batu Pahat, Johor, Malaysia

[3] Faculty of Computer Science and Information Technology (FSKTM), Universiti Tun Hussein Onn Malaysia, (UTHM), 86400 Batu Pahat, Johor, Malaysia

[4] Department of Electronic Engineering, Dawood University of Engineering and Technology, Karachi, Pakistan

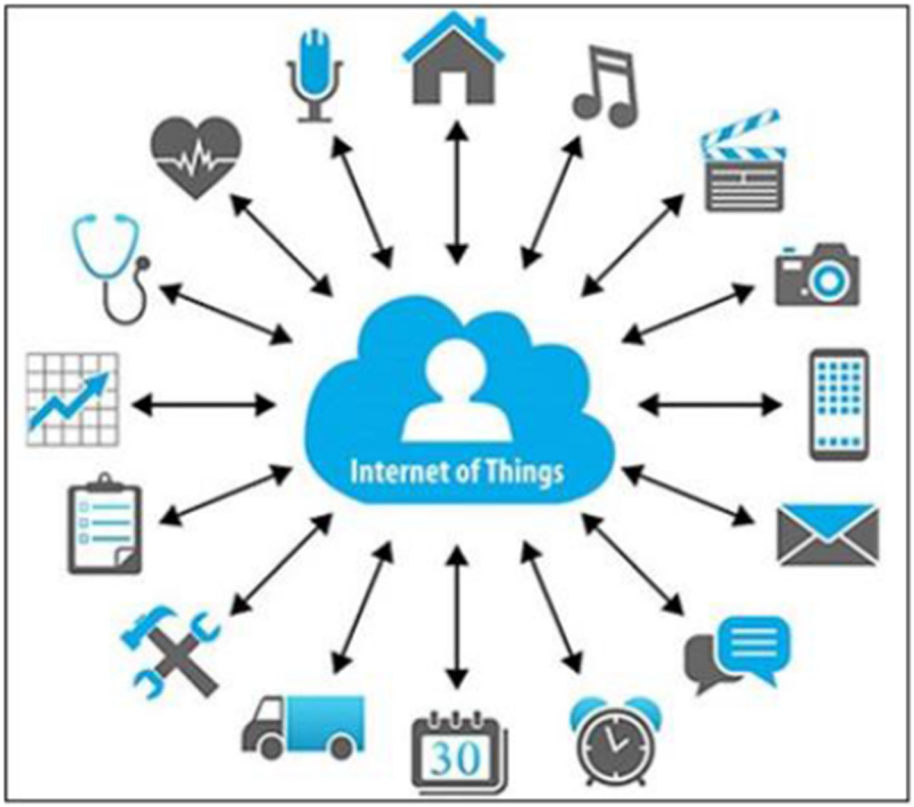

Fig. 1 Internet of Things (IoT) [3]

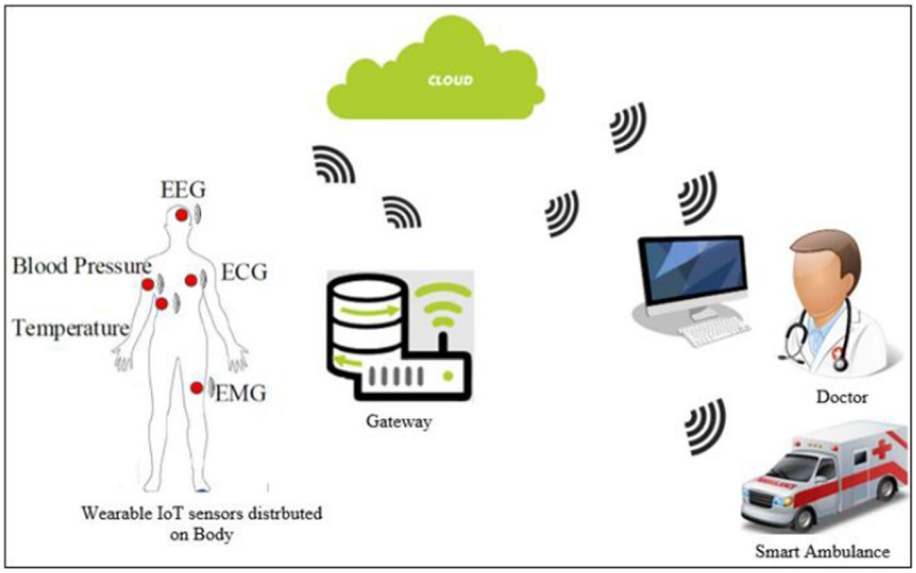

Fig. 2 The IoT-based health monitoring system architecture

assembled in IoT were required to be connected wirelessly. The right antenna design, therefore, becomes important to suits these design constraints. A small and robust antenna is needed to achieve a human-friendly, comfortable, and lightweight IoT system. The antenna should be made of a flexible material because the wearable IoT devices could work in a shape deformation environment. Besides, the antenna should have high radiation quality to promote the energy efficiency of the devices. However, the proximity of these IoT systems to lossy materials, such as the body for sensing and monitoring purposes, may be affected since the antenna's characteristics could change due to the body's high conductivity providing incorrect details. Therefore, it is necessary to ensure that the antenna can work well and that the output is stable when loading on a lossy material. Besides, it should be taken into account the effect of the

antenna on the human tissue identified by SAR will not cause any harm to our wellbeing. The SAR level should obey with the restrictions fixed by the ICNIRP and the FCC, which should be less than 2 W/kg and 1.6 W/kg above 1 g and 10 g, respectively [6].

Wearable antennas are usually embedded into clothing or attached to the body for wireless applications such as "wireless body area networks" (WBAN) for Remote Health Care Monitoring Systems [7], Doppler Radar-Based Human Vital Signs Monitoring [8], Microwave Breast Cancer Detection [9], Global Search and Rescue Satellite System [10], Steatotic Liver Detection [11], Wireless Power Transfer [12], Head Imaging [13], and Motion Capture Applications [14].

Wearable antennas, compared to traditional antennas, are considered one of the most appealing research fields due to their applications in healthcare. In the early days, researchers developed wearable antennas to work close to the body, but they discovered that the antenna's gain, efficiency, and front-to-back ratio (FBR) performance degraded as the reflection coefficient (S_{11}) shifted. They also realized that the wearable antennas emit high-back radiation, which could harm one's health. The body's high conductivity causes these drawbacks in wearable antennas. This has prompted many researchers and scientists to investigate the problem and provide the best solutions. As a result, they began to integrate the advantages of artificial structures [15–29] with wearable antennas to improve the performance of wearable antennas and keep the reflection coefficient stable.

The flexible/wearable antenna should be carefully designed so that it will not impact the human tissues when worn, and its performance should not be degraded when it is loaded on the body. Therefore, lmore than few designs have been introduced as wearable antennas for IoT systems, including loop antennas, printed Inverted-F antennas, planar monopole antennas, SIW, artificial antenna structures, and patch antennas [15–46]. However, there are few disadvantages to those designs. The designs were not conformal or low-profile as they stand out. In addition, even though the antenna was small in size, the SAR level was substandard, and the frequency can be easily detuned as the antenna was positioned on the skin of human. Some lead to an intricate design and cannot withstand a number of degrees of bending due to rigid or semi-flexible substrate.

According to the in-phase reflection behaviour of the AMC, the antenna may be located close to the AMC surface compared to the use of the PEC, which required separation of $\lambda/4$ to avoid destructive phenomena [5]. Besides, the AMC surface is also worth serving as shielding between the antenna and the tissues.

This paper aims to present a simple, durable, robust, and versatile antenna that fits into existing wearable IoT healthcare systems functioning near to the body. The antenna is considered to be a vital component of IoT's wearable healthcare systems. Since the application is wearable, we used fabric material that can be easily bent or twisted. The advantages of AMC were to ensure that the antenna has reliable performance and provide accurate information before installation in wearable IoT healthcare devices. It also protects our body from any hazel that may cause antenna radiation.

2 Antenna design

The antenna is built on a thin, flexible/wearable fabric material that has a dielectric constant of 1.9 and a thickness of 0.7 mm. A 0.17 mm thick ShieldIt^{TM} is used to construct the radiating parts such as patch, feeding and ground plane. Its conductivity is about 1.18×10^5 S/m. The presented C-shaped antenna has a size of $30 \times 30 \times 0.7$ mm^3 that is equal to $0.24\lambda_o \times 0.24\lambda_o \times 0.006\lambda_o$ mm^3, where λ_o is the wavelength in free space at the resonate frequency of 2.4 GHz.

An initial antenna design based on the principle of using a traditional shape is presented in Fig. 3a. A slot is added to form the C-shaped patch antenna as revealed in Fig. 3b. The implementation of the slot will shift the current and increases the length of its path. As a result, the S_{11} will move from higher to lower frequency bands. The impact of the slot was simulated at a resonating frequency of 2.4 GHz, as depicted in Fig. 4, to observe the surface current. This will allow us to better understand the design behavior and the part that controls the resonance frequency. It is observed that the surface current of the conventional patch is less focused on the radiated elements, as revealed in Fig. 4a. Moreover, the C-shaped slot reveals a high current, which means the critical contributor controls the resonant frequency, as shown in Fig. 4b. The C-shaped antenna is selected over the other antennas because of its simple design and can simplify the manufacturing process, especially when fabric materials are used as the substrate. Its slot on the radiator element also helps to achieve compact size.

Figure 5 reveals the S_{11} of the conventional patch, and the effect of increasing the length of the slot. The slot width was fixed at 8 mm, while continuously varies the length of the slot until it resonates at the required 2.4 GHz frequency. It can be observed that the conventional patch does not operate in the set frequency range of 2–3 GHz. However, the introduction of the C-shaped slot reduces the resonant frequency to the desired resonant frequency of 2.4 GHz. The slot length ranges from 4 to 16 mm, and the

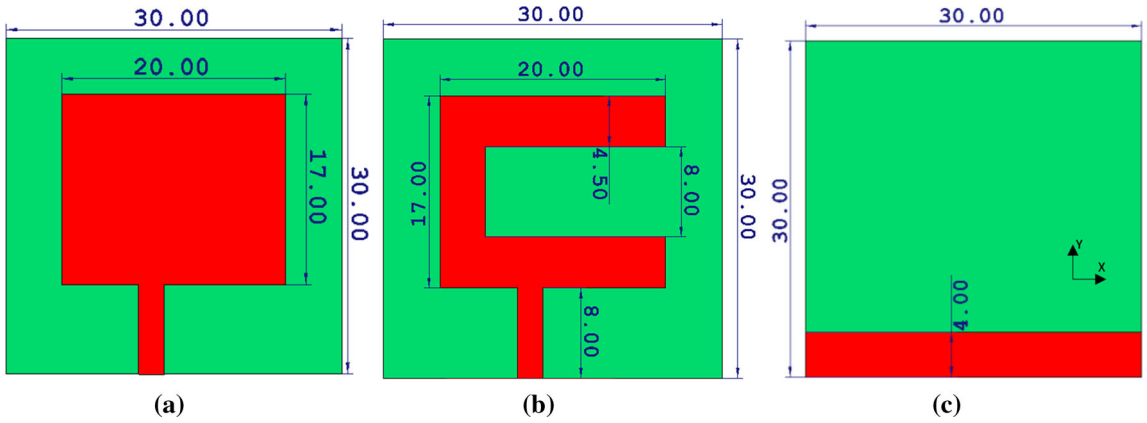

Fig. 3 **a** Conventional antenna, **b** C-shaped antenna, and **c** Back view of the conventional and C-shaped antenna

Fig. 4 Surface current distribution **a** Traditional patch, and **b** C-shaped antenna

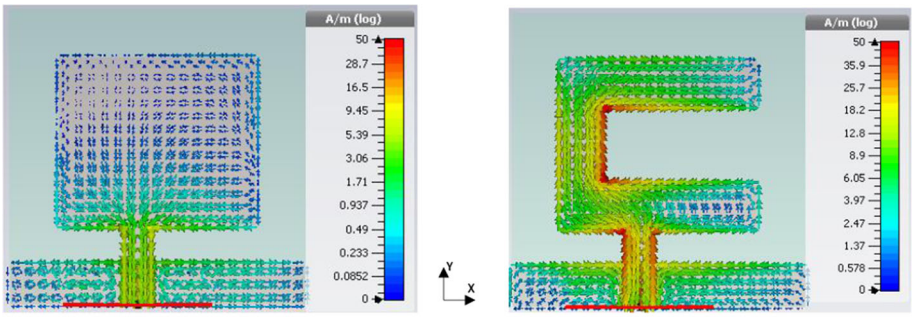

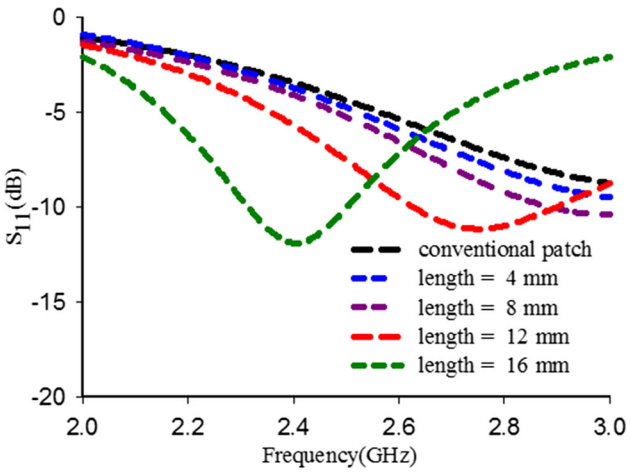

Fig. 5 S_{11} of the conventional patch and the impact of increasing the slot length

resonance frequency is observed to decrease sharply as the length increases, as shown in Fig. 5.

As the antenna presented for the application of wearable IoT healthcare devices, it is necessary to examine the antenna performance before being integrated into the system in order to ensure its stable performance. Therefore, the antenna was simulated on four multilayer human body tissues consists of muscle (thickness = 20 mm, $\sigma = 1.77$ (S/m),$\varepsilon_r = 52.67$, density = 1006 kg/m^3), fat (thickness = 5 mm, $\sigma = 0.11$ (S/m),$\varepsilon_r = 5.27$, density = 900 kg/m^3), bone (thickness = 13, mm $\sigma = 0.82$ (S/m),$\varepsilon_r = 18.49$, density = 1008 kg/m^3), skin (thickness = 2 mm $\sigma = 1.49$ (S/m), $\varepsilon_r = 37.95$ density = 1001 kg/m^3) [5]. Multilayer human body tissues were formed in a square, and a cylinder-shaped represented as the chest and arm, respectively, as shown in Fig. 6. The square (chest) has an overall dimension of $150 \times 150 \times 40$ mm^3, while the cylinder (arm) has a length of 150 mm and a diameter of 80 mm [6].

Figure 7 shows the performance of the C-shaped antenna mounted on the chest and arm. It has been known that its resonance frequency is detuned and does not work in the desired frequency range. Therefore, to ensure the stable performance of the presented C-shaped antenna on the human body, the AMC structure is introduced, which can reduce the interaction between the C-shaped antenna and the tissues.

3 AMC design

AMC is an engineering substance that can act as a PMC that cannot be found by nature. Compared to the PEC whose incident wave of 180° reflection phase, the AMC

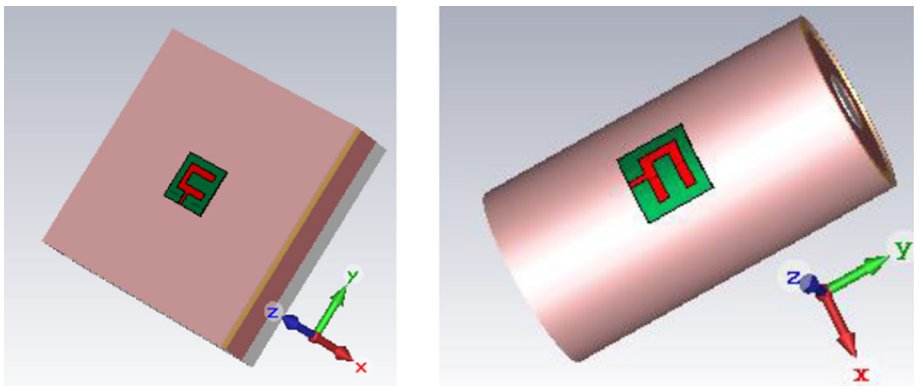

Fig. 6 Phantoms models developed in CST **a** Chest human model, and **b** Arm human model

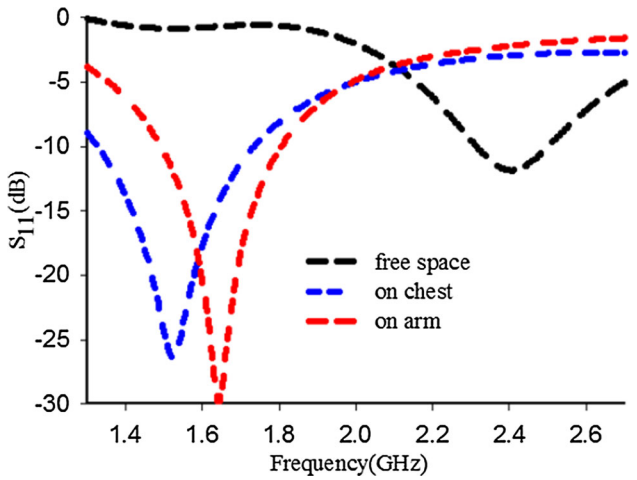

Fig. 7 S_{11} of the C-shaped antenna loading on chest and arm and in free space

incident wave has a 0° reflection phase characteristic of the imitative PMC behavior. Figure 8 demonstrates the structure of the AMC and the PEC, which are positioned near a radiator that could be an antenna. When the antenna is set on a metal ground plane, and the distance between the antennas is less than λ/4, its 180° reflection phase can cause destructive interference with forwarding radiation, resulting in poor performance, thereby reducing overall efficiency. This is due to the current cancellation caused by the direction opposite to the original current and the current image. However, when the antenna is located on the AMC structure, and the distance between the antenna is much shorter than λ/4, the 0° reflection phase of the antenna can cause constructive interference with the forward radiation. Therefore, the AMC will guide both the image and the original currents to have the same direction, resulting in good performance and efficiency. Besides, the AMC structure can protect the antenna from deterioration of the body, maintain good efficiency and keep more radiation away from the body. On the other side, the use of PEC requires a thick substrate with a thickness equal to or greater than λ/4 [6]. As a result, the antenna maintains a large lateral size.

The final optimized AMC cell configuration is shown in Fig. 9. It is built on the same substrate as the antenna but has a thickness of 2.2 mm. The unit cell has a dimension of $27 \times 27 \times 0.7$ mm^3, which is equal to $0.22\lambda o \times 0.22\lambda o \times 0.006\lambda o$ mm^3, where the wavelength in free space at the resonant frequency of 2.4 GHz. Numerical simulation is performed based on CST Microwave Studio software to characterize the performance of the presented AMC unit cell structure. The unit cell is simulated as an infinite sequence using periodic boundary conditions along the x- and y- directions. The unit cell was excited in the positive z-direction using a plane-wave excitation while the perfect electric ($E_t = 0$) was placed in the negative z-direction by the full metallic sheet.

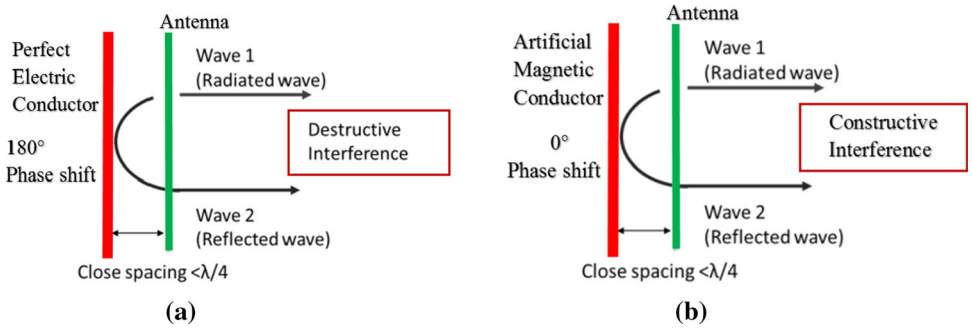

Fig. 8 Concepts of the position the antenna on Reflector **a** PEC, and **b** AMC structures [6]

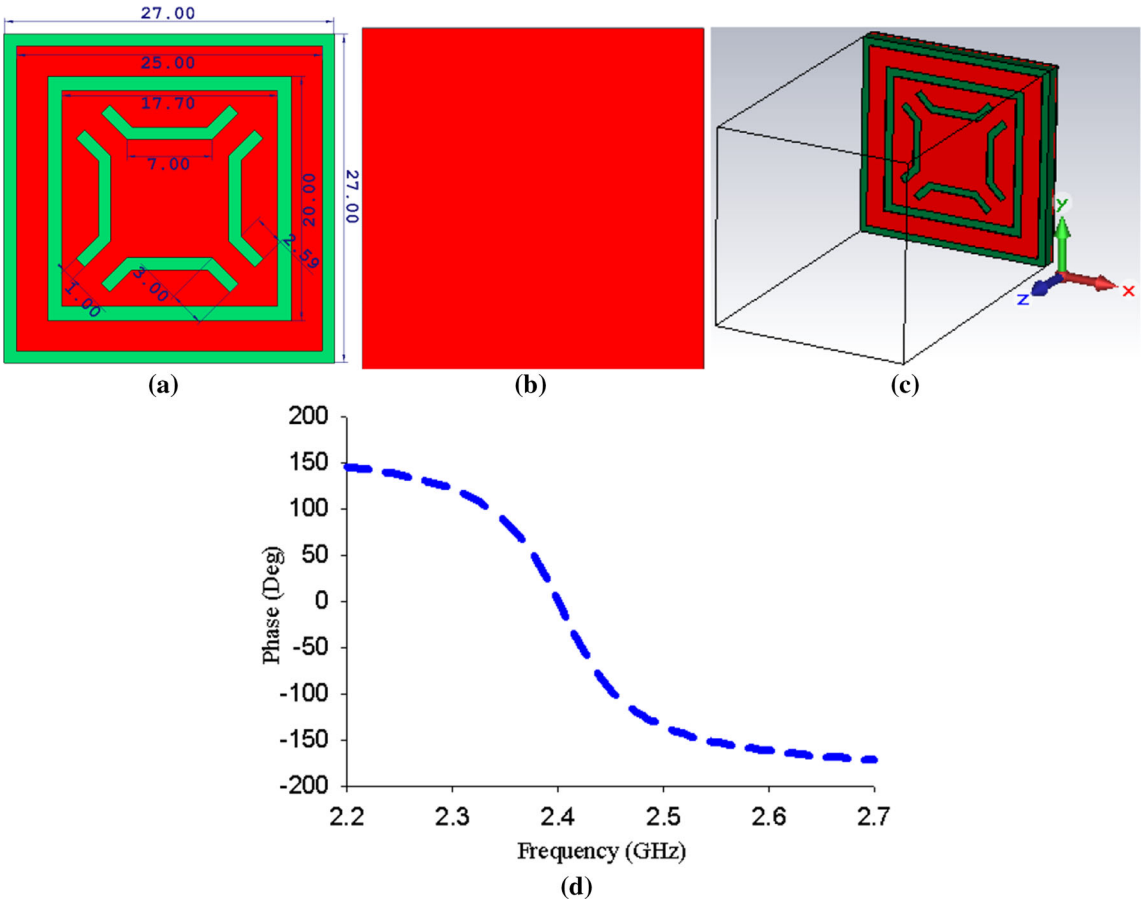

Fig. 9 AMC unit cell and it's characteristic **a** Front-view, **b** Back-view, **c** Perspective-view, and **d** Reflection phase

The square and the symmetric slots are used to reduce the size of the AMC. The slots can increase the path current that corresponds to shifting the phase to a lower frequency band. Figure 9d presents the reflection phase of the final optimized AMC unit crossing zero degrees at the desired frequency of 2.4 GHz. At this frequency, the AMC can alleviate the impact of impedance mismatch resulting from the characteristics of the body tissue, increases the gain, and decreases the back lobe of the antenna. The AMC structure also plays a crucial role in minimizing the thickness of the presented antenna profile. It also minimize the coupling between that caused the antenna and the human body, making it ideal for enhancing the efficiency of flexible/wearable antennas.

4 Performance of the antenna with AMC

4.1 Design configuration

The configuration of the introduced combined design and the prototype are depicted in Figs. 10 and 11, respectively. It consists of three layers: a C-shaped antenna, 2 × 2 AMC structures, and a Styrofoam layer, as shown in Fig. 11a. The Styrofoam layer is used to isolate the antenna from AMC structures to prevent any interaction between them. The overall dimension of the integrated design is $54 \times 54 \times 3.9$ mm^3 which is equal to $0.43\lambda o \times 0.43\lambda o \times 0.03\lambda o$.

4.2 Investigation of the C-shaped antenna added to AMC in free space

When the C-shaped antenna is integrated with the presented AMC, there will be a mutual impedance coupling between the two elements that result resonance detuning. Thus, to get the required resonant frequency, the size of the C-shaped antenna is slightly altered when integrated with the AMC structures. The modified dimension is shown in Fig. 10. The simulated and measured results of the return loss for the integrated C-shaped antenna with the AMC structures are shown in Fig. 12. The result shows that simulated and measured resonances are generally agreed.

The radiation patterns of the added AMC structures to the presented C-shaped antenna and the C-shaped antenna alone are carried out along E-plane and the H-plane.

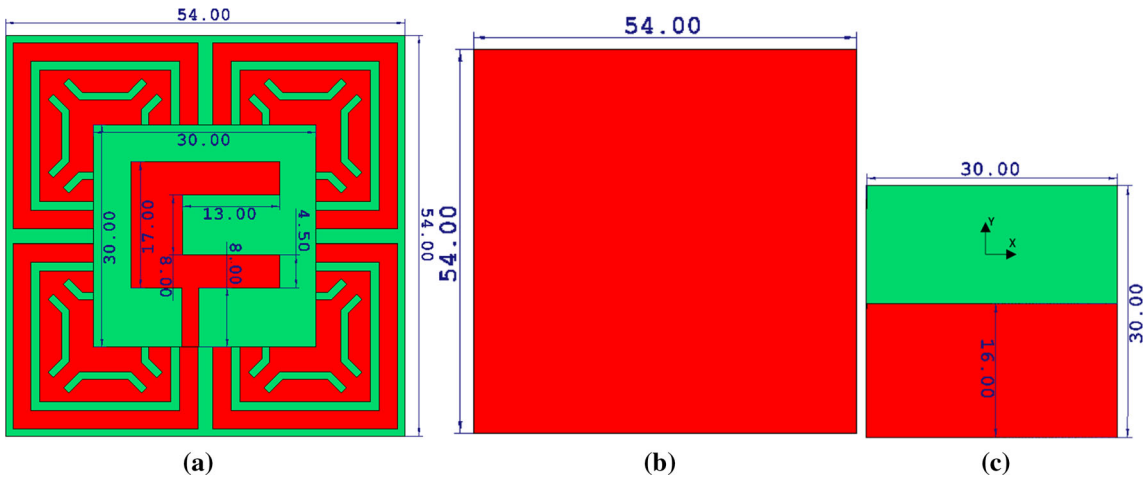

Fig. 10 Configuration of the added AMC structures to C-shaped antenna **a** Front-view of the integrated design, **b** Back-view of AMC structures, and **c** Back-view of the C-shaped antenna

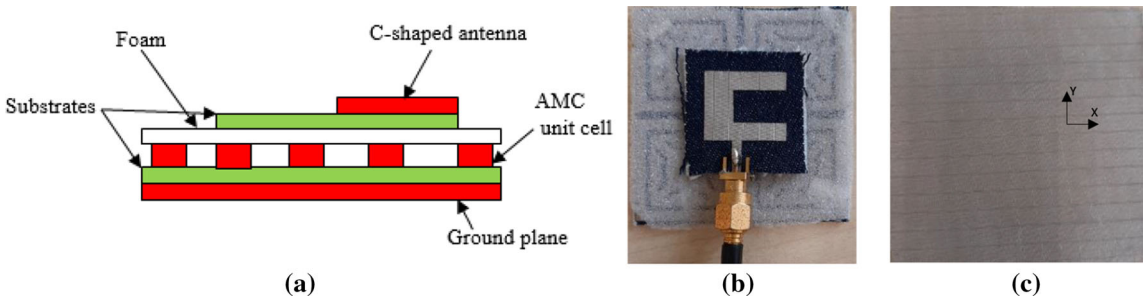

Fig. 11 **a** Side view of the integrated C-shaped antenna, **b** Front-view of the fabricated design, and **c** Back-view of the fabricated design

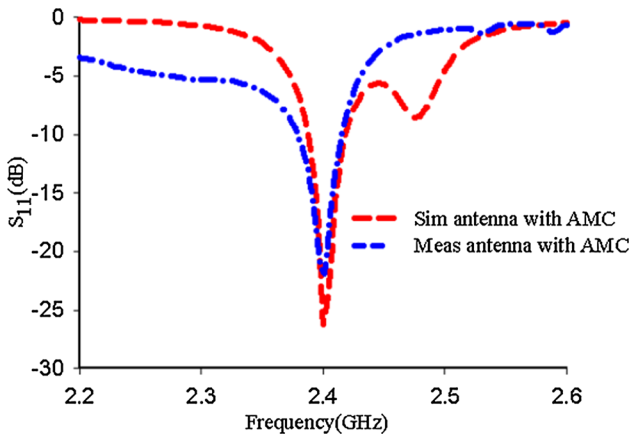

Fig. 12 Simulated and measured S_{11} of the integrated C-shaped antenna with AMC

Figure 13a shows that the C-shaped antenna has dipole-like radiation characteristics along the E-plane, while the Omni-directional has a long H-plane. This form of radiation is not desired for body applications due to back radiation that may cause harm to our health. Figure 13b demonstrates the radiation pattern of the C-shaped antenna added to the AMC structures. It is seen that the AMC has caused apparent changes in the direction of the antenna. It leads to significant FBR and reduces backward radiation, which is desirable to the body application. The reduction is approximately 13.8 dB. It as well enhanced the gain from 1.28 to 6.49 dB (as revealed in Fig. 13c and d) in a direction away from the body, thereby showing the benefit of the AMC when integrated with the C-shaped antenna. The measured result shows a slight difference from the simulated, which may be attributed to the measurement environment, such as cables, connections, manufacturing errors.

4.3 Investigation of the C-shaped antenna added to AMC under bending

In the case of bending, one of the essential factors for wearable IoT devices is the performance of the proposed design. Maintaining the design flat in the human environment is a challenge, particularly for components made of highly flexible materials. It is therefore essential to study

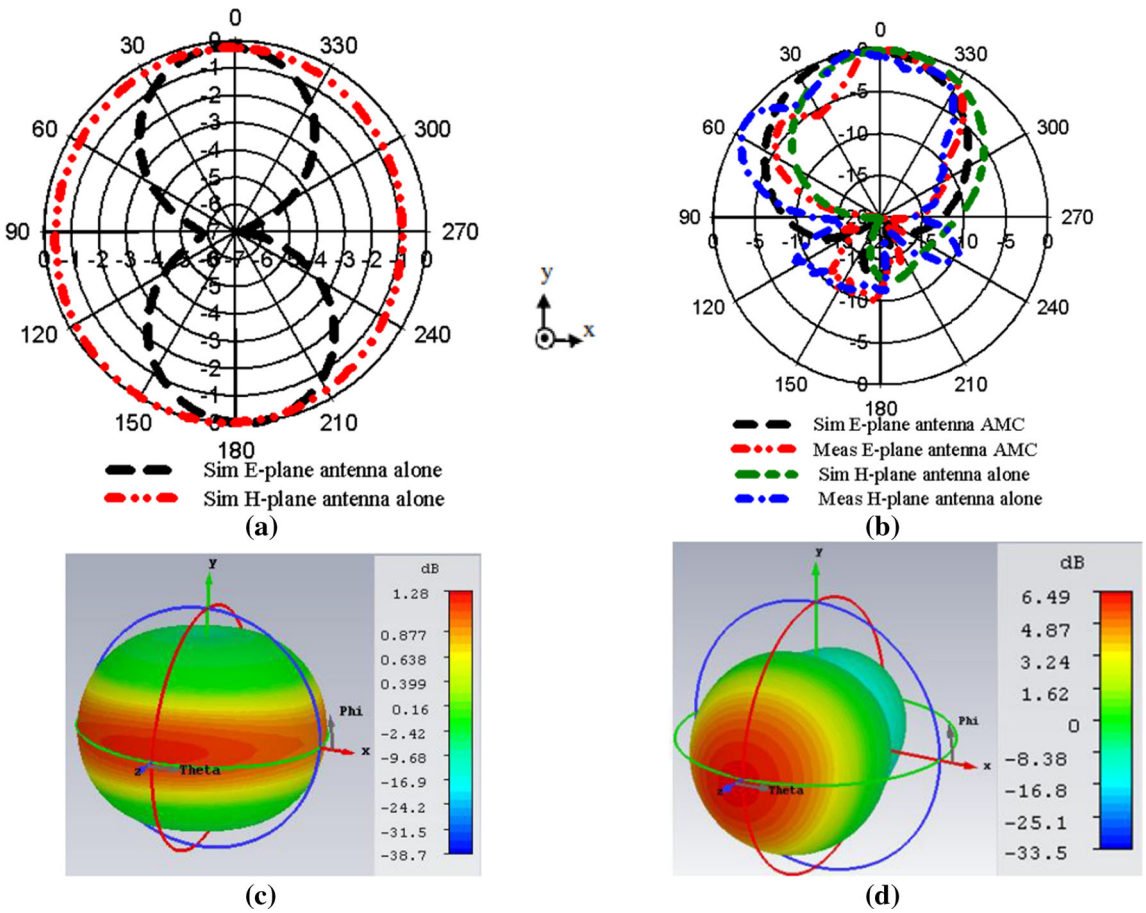

Fig. 13 Fairfield result **a** Radiation pattern of the C-shaped antenna alone, **b** Radiation pattern of the C-shaped antenna alone with AMC, and **c** Gain of the C-shaped antenna alone, and **d** Gain of the C-shaped antenna with AMC

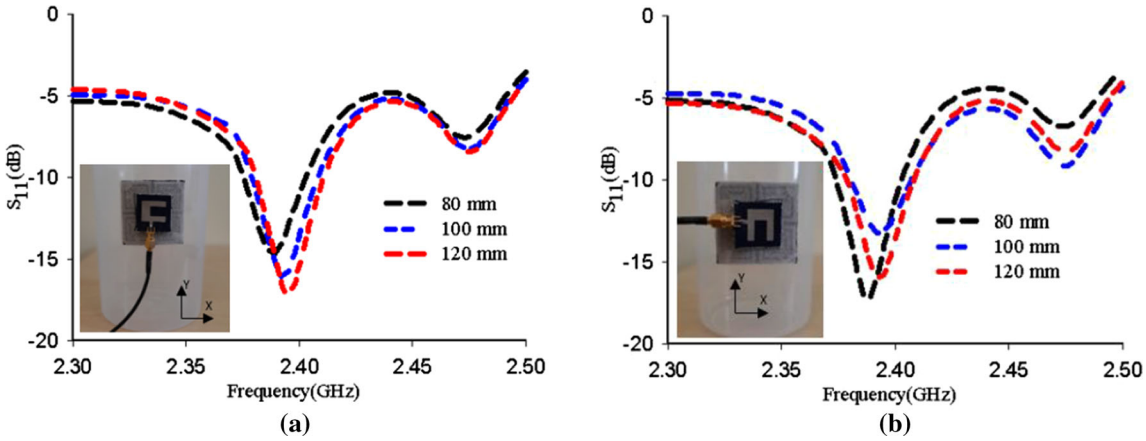

Fig. 14 Measured S_{11} of the presented C-shaped antenna added to the AMC structure under bending **a** y-axis, and **b** x-axis

the efficiency of the proposed design under bending scenarios. The design is mounted curved along the x-axis and the y-axis. Three diameters are used to evaluate the performances (80 mm, 100 mm and 120 mm), which approximately equal to the scale of the human arm and leg. A very thin tape was used to fix the design of the cylinder.

Figure 14 displays the measured reflection coefficient, S_{11} bending results for two axes. From the figure, it is observed that the desired frequency band is still within a bandwidth of -10 dB. In both cases, a slight resonance shift may be caused by the use of a plastic cylinder model with a

dielectric constant greater than one or may be caused by the effect of bending along the stripline.

4.4 Investigation of the C-shaped antenna added to AMC loading on a body

The human body is considered a complex structure due to its shape and high conductivity. Therefore, it is necessary to examine the performance of the presented C-shaped antenna with and without AMC structures before being assembled into the wearable system to ensure its stable performance. Both designs are evaluated using the developed phantom models presented in Sect. 2.

The C-shaped antenna with and without AMC structures was mounted directly and indirectly on the chest and arm. The findings are shown in Figs. 15 and 16. Figure 15 shows that the output of the C-shaped antenna without AMC structures is significantly degraded when operated on biological phantom models. Interference between the model of the human body and the C-shaped antenna causes impedance mismatch. The reflection coefficient, S_{11} fell significantly as the antenna was closed to the phantom models. In this situation, the interaction between the C-shaped antenna and the phantom models is severe, so it is vital to find a solution to reduce the influence of the phantom models. As a result, the C-shaped alone is not suitable for assembly in any wearable device.

Meanwhile, Fig. 16 indicates the S_{11} of the two phantom models are constant for integrating C-shaped with the AMCs. It reveals that the AMC structures formed a good insolation layer between the C-shaped antenna and the phantom versions. In addition, to corroborate with the simulated results, the integrated C-shaped antenna with AMCs was further investigated in a real human body. The design was placed on the arm, chest, and back, as shown in Fig. 17. Figure 18 indicates the coefficient of reflection, $S_{11,}$ at three positions. It can be shown that the desired frequency of resonance is maintained. There was also a slight resonance shift in the arm, which may be attributed to the bending behavior caused by the curved structure of the arm.

The radiation pattern of the C-shaped antenna with and without AMC is also being studied. The designs were placed in the same positions on the phantom models, as shown in Figs. 15 and 16. Figure 19 shows the far-field result for the C-shaped antenna alone cases. It can be seen clearly that the back radiation is significantly decreased relative to the case without the body. This means that the human body absorbs much energy that can cause damage to the tissues and impair blood circulation. This is due to that the body behaves as an extra substrate; thus, positioning the presented C-shaped antenna on the human skin created a significant disparities in the antenna's results. The gain performance is affected with the gain value is reduced from 1.28 dB (see Fig. 13c) to − 9 dB (see Figs. 19c and d).

Loading AMC structures with a C-shaped antenna showed a comparable radiation pattern for both body and without body, as shown in Fig. 20. There is a slight difference in design loading on phantom models in terms of gain and backward radiation, but this is not significant. The AMC structures greatly benefit from achieving high-level stability results, such as resonance frequency, gain, FBR, efficiency. This indicates that the AMC structures have formed a good layer of isolation between the antenna and the body.

Further investigation is carried out to compare the FBR and the efficiency of the C-shaped antenna alone in a free space and on the phantom versions. The findings are shown in Fig. 21. Figure 21 shows that the C-shaped antenna

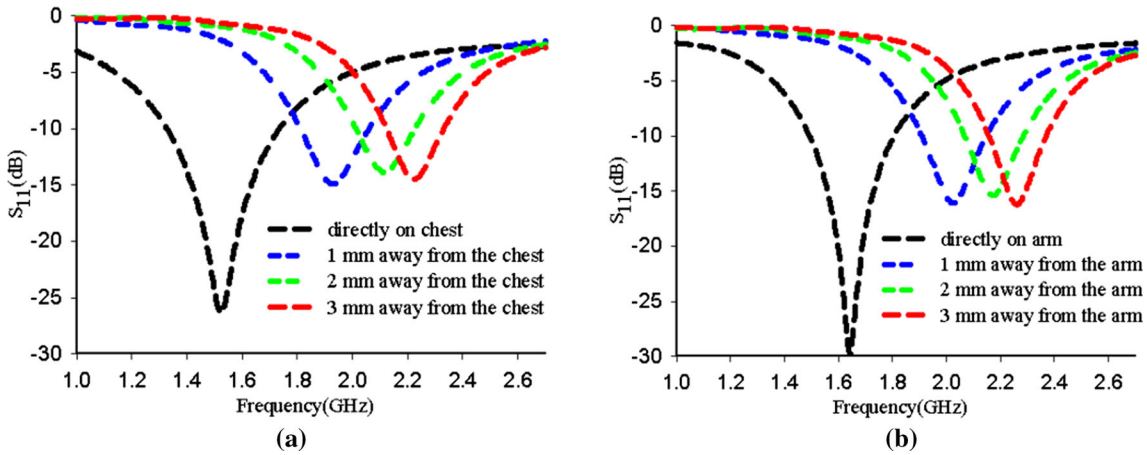

Fig. 15 S_{11} of the loading C-shaped antenna alone on the body **a** on chest, and **b** on arm

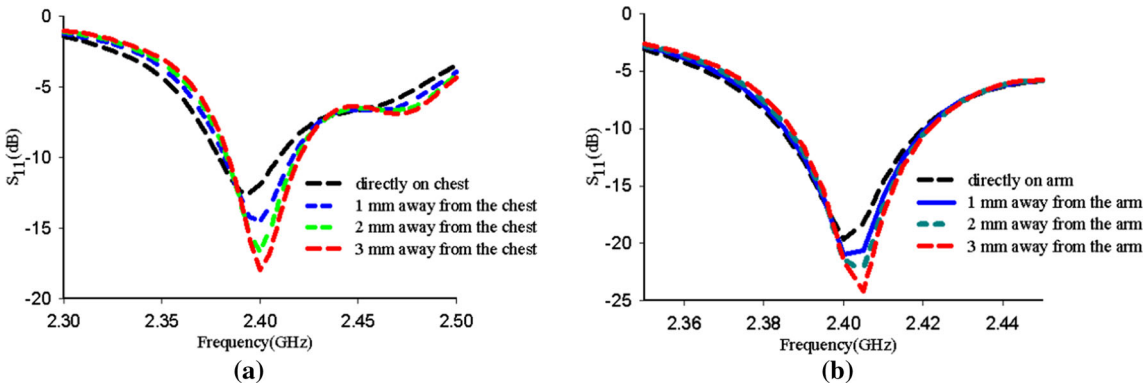

Fig. 16 S_{11} of loading the C-shaped antenna with AMC structures on the body **a** on chest, and **b** on arm

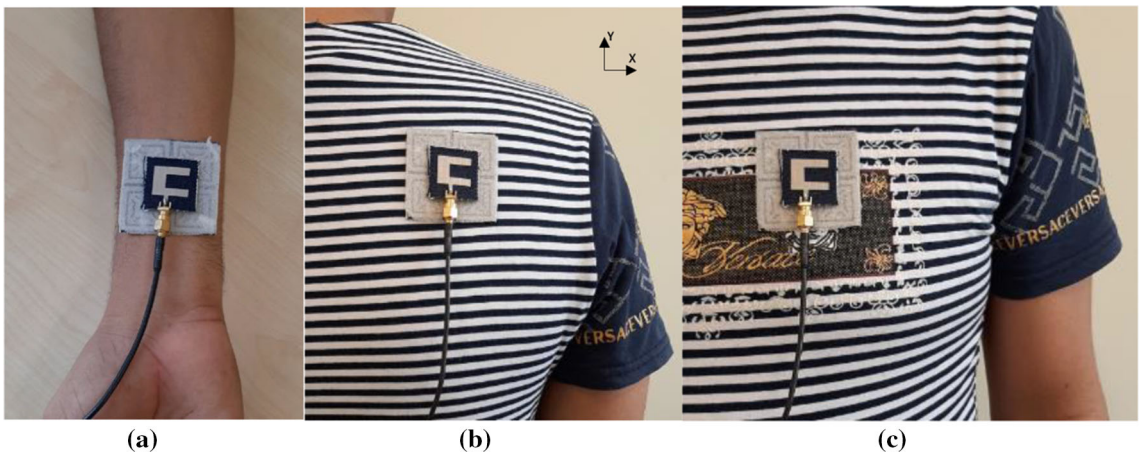

Fig. 17 C-shaped antenna integrated with AMC on the real human bod **a** Chest, **b** Back, and **c** Arm

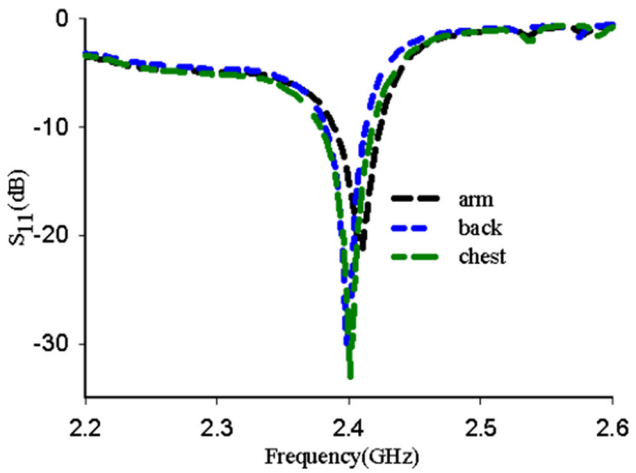

Fig. 18 Measured S_{11} of the loading C-shaped antenna with AMC structures on the real human body

shows 0 FBR when operating in free space, suggesting high back-lobe radiation. On the other hand, when the C-shaped antenna is on the body, the FBR rises by about 13.3 for the arms and about 14.5 for the chest. Compared to free space, the rises are since the body serves as a substrate and absorbs energy that can cause health problems. The efficiency of the C-shaped antenna in free space shows an excellent performance of 90%, and when it is loaded into the body, the efficiency is almost reduced to 10%.

The FRB and the efficiency of the AMC with a C-shaped antenna were also studied on the chest and arm of the human body models and free space, as shown in Fig. 22. It can be noticed that there is not much difference between FBR on the chest and arm load and free space. The difference shall not exceed 2 dB. It can also be shown that there is no apparent difference in the efficiency of the chest and arm load and free space. The results of FBR and efficiency are comparable on the chest and arm load and free space, suggesting that the AMC structure will serve as a shielding layer between the C-shaped antenna and the body so that the C-shaped antenna can function equally well, whether it is placed on the body or in free space.

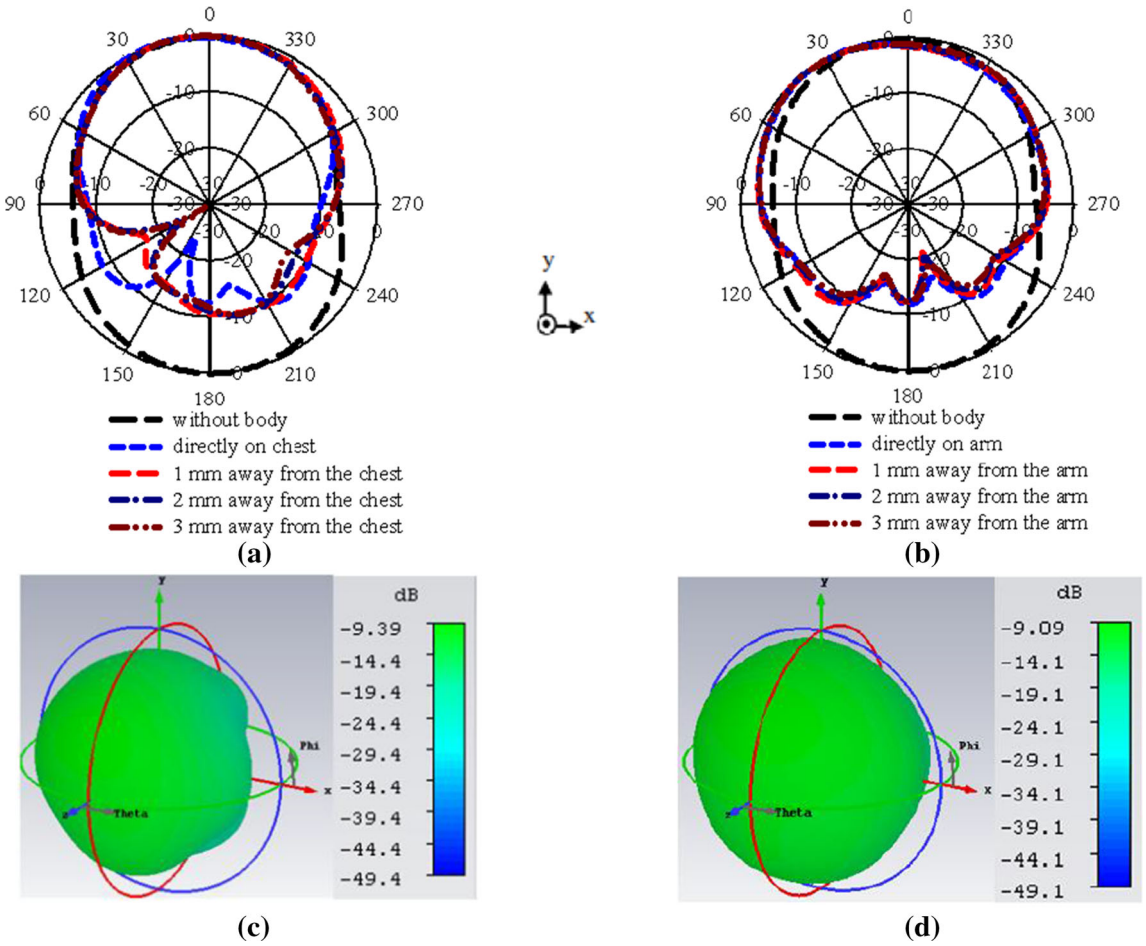

Fig. 19 Far-field result of C-shaped antenna on body **a** radiation pattern on the chest, **b** radiation pattern on the arm, and **c** gain on the chest, and **d** gain on the arm

4.5 Specific absorption rate (SAR)

Due to the health risks of electromagnetic radiation to the body, the C-shaped antenna SAR with and without AMC structures must be evaluated. The same chest and arm models used in Sect. 2 are utilized for the Specific Absorption Rate evaluation. As a benchmark, an input power of 100 mW was selected for the presented C-shaped antenna with and without AMC. The SAR was determined according to the IEEE C95.1 standard given in the CST. The SAR levels were compared with ICNIRP and the FCC, which were to be less than 2 W/kg and 1.6 W/kg above 1 g and 10 g of organic tissue mass. The SAR level was studied by placing the design directly on the skin and with a spacing of 1, 2 and 3 mm far from the phantom models. Table 1 summarizes the C-shaped antenna SAR levels. It is shown that the SAR level exceeds the limits set by the standards, even when the C-shaped has spacing of 3 mm far from the chest and arm human body models.

On the other hand, the addition of AMC structures to the C-shaped antenna shows a significant reduction in the SAR level of the two standards, even when positioned directly on the skin of the human body as tabulated in Table 2. The reduction is more than 90 compared to the C-shaped antenna alone. Figures 23 and 24 display the 3-D SAR results based on 1 g of the C-shaped antenna with and without AMC, respectively. The designs are placed directly on the phantom models. Figure 23 shows the reduction of the SAR below the safety limit (1.6 W/kg) when AMC is integrated with a C-shaped antenna; otherwise, the SAR level exceeds the safety level (1.6 W/kg) as depicted in Fig. 24.

5 System implementation based on wireless body area network related to the current pandemics

Wireless Body Area Network (WBAN) systems have been used in various applications, especially in medical applications, because they continuously monitor multiple sensors such as blood glucose, oxygen levels, blood pressure,

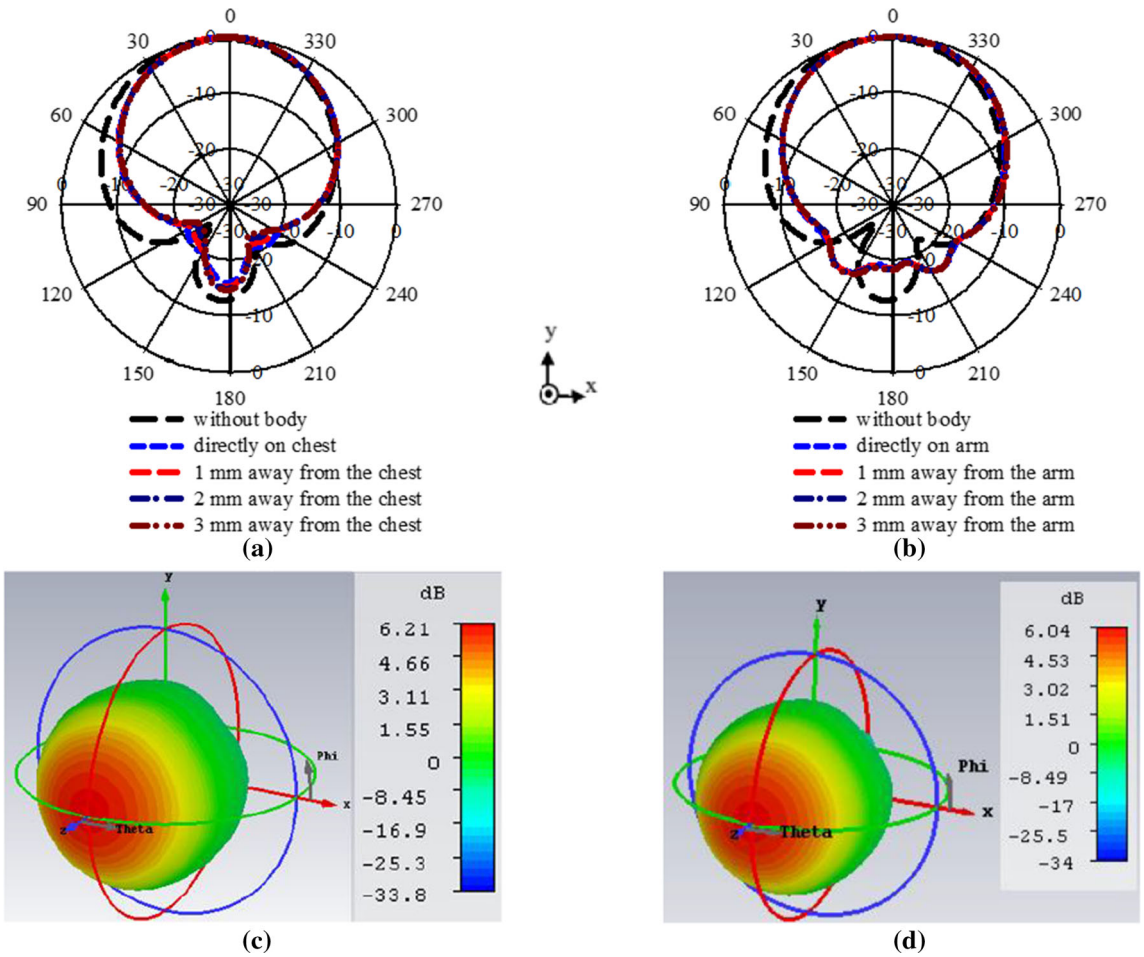

Fig. 20 Fairfield result of C-shaped antenna with AMC structures on body **a** Radiation pattern on chest, **b** Radiation pattern on arm, and **c** Gain on chest, and **d** Gain on arm

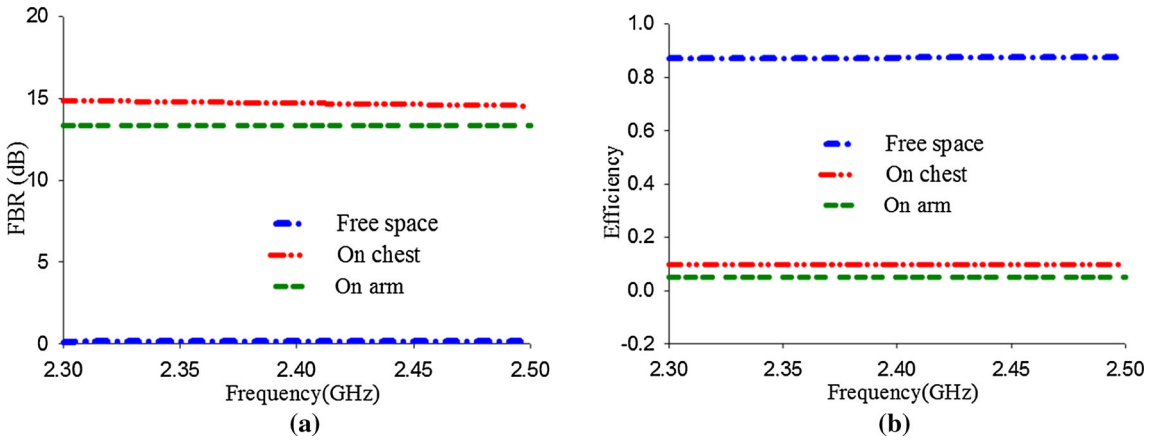

Fig. 21 Performance of C-shaped antenna alone on phantom models and free space **a** FBR, and **b** Efficiency

and heart rate. These sensors are connected to a wearable antenna to collect information from the patient and transmit it directly to the general practitioner (GP). The information will be transmitted to the cloud through the gateway and then transmitted to the doctor. The wearable antenna can be positioned close to the patient's body or can be a part of his clothes. Therefore, integrating wearable devices into clothes is the perfect way to achieve ubiquitous and continuous health monitoring. The wearable antenna presented in this paper aims to remotely monitor patient's health in

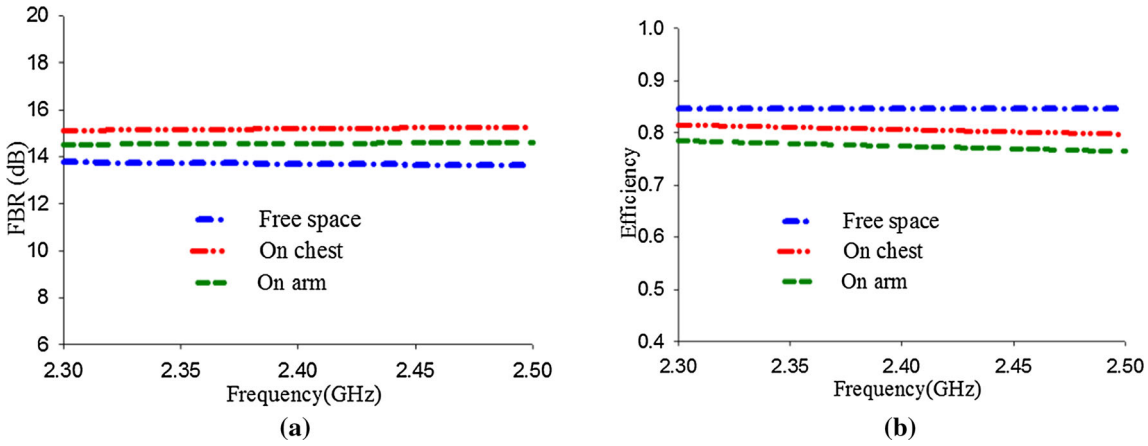

Fig. 22 Performance of C-shaped antenna with AMC structures on phantom models and free space **a** FBR, and **b** Efficiency

Table 1 SAR values over 1 g and 10 g the C-shaped antenna alone

Position of the design	Chest		Arm	
	1 g	10 g	1 g	10 g
Directly on skin	15.2	4.51	11.3	4.09
1 mm away from skin	8.63	2.99	8.2	8.2
2 mm away from skin	7.47	2.84	7.39	3.43
3 mm away from skin	6.6	2.65	6.65	3.19

Table 2 SAR values over 1 g and 10 g the C-shaped antenna with AMC structures

Position of the design	Chest		Arm	
	1 g	10 g	1 g	10 g
Directly on skin	0.807	0.4	0.555	0.292
1 mm away from skin	0.649	0.277	0.494	0.223
2 mm away from skin	0.491	0.213	0.523	0.268
3 mm away from skin	0.424	0.177	0.548	0.311

the hospital or at home. Wearable antennas will collect the information from the distributed sensors on the patient's body and transmit it to the general practitioner (GP) or health centers. The information will be processed and assessed through the system. Decisions will be made based on these assessments of whether warnings should be sent or not. For example, if one of the vital signs increases, such as blood pressure, the sensor will read the value and send it to the GP through the wearable antenna. Another example that is now considered very important is monitoring oxygen levels due to the covid 19 pandemics. Overcrowded hospitals require patients to stay home. Therefore, it is very important to monitor and locate the patient. With the help of wearable antennas, we can continuously monitor patients and send data regularly. The proposed antenna's process to control the patient's vital signs in the smart healthcare system is shown in Fig. 25.

6 Conclusion

A wearable fabric C-shaped antenna operating on the 2.4 GHz ISM band for wearable IoT healthcare devices is presented. The design began with a conventional antenna, and a slot was added to form a C-shaped antenna. The function of the slot was to divert current and increase its path, which corresponds to the reduction in size. The C-shaped antenna was loaded onto the body to ensure that its output was reliable before being reassembled into a flexible/wearable devices in which the antenna is considered to be a central part of the system. The C-shaped antenna demonstrated an unstable reflection coefficient, meaning that the antenna does not function under the desired band. Therefore, it is not recommended to mount a C-shaped antenna in a wearable IoT system that operates near the human body. However, the advent of AMC structures has overcome this problem, which can mimic the output of PMC. The total size is $54 \times 54 \times 3.9$ mm^3, which is equal to $0.43\lambda o \times 0.43\lambda o \times 0.03\lambda o$, where the wavelength in free space at the resonate frequency of 2.4 GHz. The AMC structures serve as a shielding layer between the C-shaped antenna and the body, allowing the C-shaped antenna to function equally well, whether on the body or in free space. When the C-shaped antenna is mounted on the chest, the performance decreases. For example, the gain is reduced from 1.28 to − 9 dB, and the

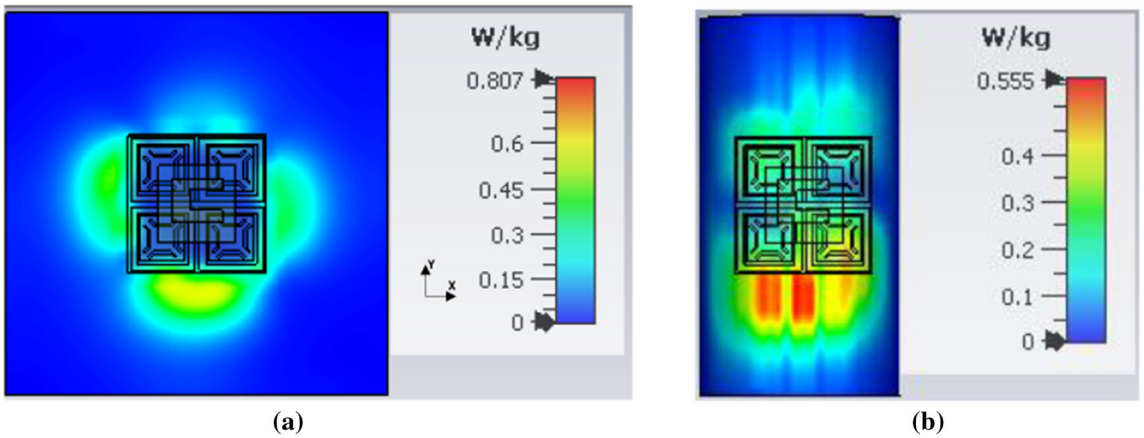

Fig. 23 3D SAR results based on 1 g of the C-shaped antenna with AMC structures placed directly on the phantom models **a** on the chest and **b** on the arm

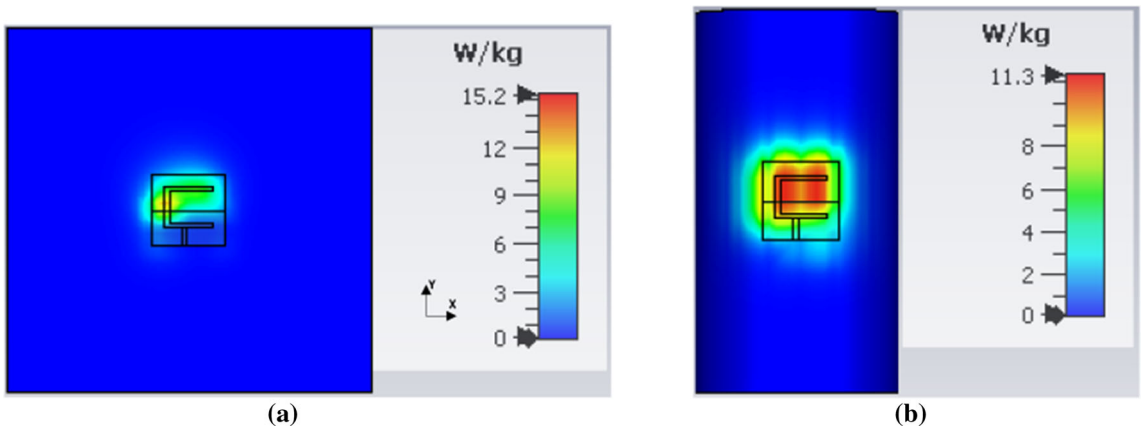

Fig. 24 3D SAR results based on 1 g of the C-shaped antenna alone placed directly on the phantom models (a) on the human body chest, and (b) on the human body arm

efficiency decreases from 90 to 10%. The addition of the AMC structure demonstrated excellent performance in terms of efficiency and gain. The gain and efficiency without and with chest are 6.49 dB, 84% and 6.21 dB, and 81%, respectively. The results revealed that with the inclusion of the AMC, the SAR levels were decreased by more than 90% between the FCC and ICNIRP standards compared to the C-shaped antenna alone. The integrated AMC with a C-shaped antenna was mechanically robust in terms of deformation and loading of human tissue. As a result, the integrated C-shaped with AMC structures is highly suitable for assembly in any wearable IoT healthcare device. Finally, the output of the C-shaped antenna with and without AMC Structures is summarized, as shown in Table 3. Furthermore, Table 4 compares the performance of the introduced flexible antenna design with works published in the past two years. It can be observed that the presented integrated design shows excellent performance. Future work focuses on implementing the design in real applications in the IoT as a sensor for transferring the data from the patient to the doctor, battlefield survival, personalized health care systems, emergency and tracking rescue systems.

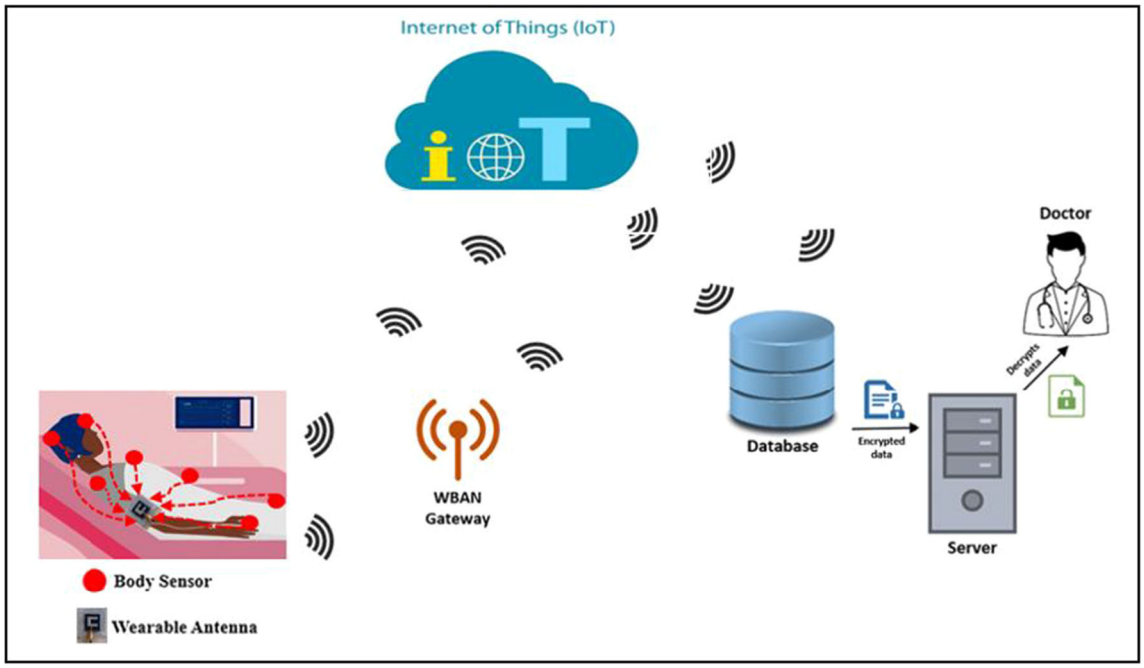

Fig. 25 Wireless body area network (WBAN) architecture of healthcare applications

Table 3 Comparision between C-shaped antenna alone and with AMC strctures

Performance	Free space		On chest	
	C-shaped antenna	C-shaped antenna with AMC strctures	C-shaped antenna	C-shaped antenna with AMC strctures
S_{11}	Stable	Stable	Shifted	Stable
Gain (dB)	1.28	6.49	− 9	6.21
Efficency (%)	90	84	10	81
FBR (dB)	0	13.8	14.5	15.2

Table 4 Comparison of previous work with presented design at 2.4 GHz

Refs.	Year	size of proposed design (mm^3)	Type of substrate	No. of unit cells	Gain (dBi)	Efficiency (%)	FBR (dB)	SAR W/kg
[17]	2018	81 × 81 × 4	Fabric	3 × 3	7.3	71	17	0.230
[18]	2019	66.8 × 66.8 × 5	Polyimide	2 × 2	7.47	–	20	0.15
[19]	2020	75.7 × 75.7 × 6.1	Felt & Ultralam3850	3 × 3	6.379	38.84	14	0.022
[20]	2020	60 × 60 × 8.5	PDMS	3 × 3	6.56	70.7	–	0.612
[21]	2020	145 × 112 × 3.424	Jeans	4 × 3	6.19	61	–	–
[22]	2020	50 × 25.7 × 5	Felt	1 × 2	4.06	44.39	–	0.521
[23]	2020	120 × 120 × 3.6	Leather & textile	3 × 3	7.98	86.2	–	0.21
[24]	2020	60 × 60 × 2.4	Fabric	2 × 2	6.45	–	16	0.983
[25]	2020	85.5 × 85.5 × 5.28	Felt	3 × 3	1.94	–	12	0.111
[26]	2020	55.79 × 52.25 × 4.5	Substrate(2.65)	3 × 3	4.25	88	2.1	0.65
[27]	2020	70 × 85 × 6	Felt	–	8.3	49	–	–
[30]	2020	35 × 35 × 8.508	Rogers 4003C	–	7.2	80	18.2	0.17
[28]	2021	56 × 56 × 6	Ultralam850 & Felt	2 × 2	6.51	74.8	11.4	0.22
Our paper	2021	54 × 54 × 3.9	Fabric	2 × 2	6.49	84	13.8	0.649

Declarations

Conflict of interest The Authors and Co-Authors have no conflicts of interest. The paper is not submitted to any other Journals. This is solely submitted to this Journal.

Ethical Approval The institute of integrated Engineering Health committee of Universiti Tun Hussein Onn Malaysia waived the need for ethical approval. The participant was voluntary and gave verbal informed consent.

References

1. Al-Sehemi, A., Al-Ghamdi, A., Dishovsky, N., Atanasova, G., & Atanasov, N. (2020). A flexible broadband antenna for IoT applications. *International Journal of Microwave and Wireless Technologies, 12*(6), 531–540.
2. Mohamed, H. A. and Sultan, K. S. (2018). Quad Band Monopole Antenna for IoT Applications. In *2018 IEEE International Symposium on Antennas and Propagation & USNC/URSI National Radio Science Meeting*, no. c, pp. 1015–1016.
3. Internet of Things. [Online]. Available: https://semielectronics.com/sensors-lifeblood-internet-things/
4. Kumar, S., Buckley, J. L., Barton, J., Newberry, R., Dunlop, G., Rodencal, M., & O'Flynn, B. (2019). A bandwidth enhanced 915 MHz antenna for IoT wrist-watch applications. In *2019 13th European Conference on Antennas and Propagation (EuCAP)* (pp. 1-5). IEEE.
5. Di Serio, A., Buckley, J., Barton, J., Newberry, R., Rodencal, M., Dunlop, G., & O'Flynn, B. (2018). Potential of sub-GHZ wireless for future IoT wearables and design of compact 915 MHz antenna. *Sensors, 18*(1), 22.
6. Ashyap, A. Y., Dahlan, S. H. B., Abidin, Z. Z., Abbasi, M. I., Kamarudin, M. R., Majid, H. A., & Alomainy, A. (2020). An overview of electromagnetic band-gap integrated wearable antennas. *IEEE Access, 8*, 7641–7658.
7. Corchia, L., Monti, G., De Benedetto, E., & Tarricone, L. (2017). Wearable antennas for remote health care monitoring systems. *International Journal of Antennas Propagation, 2017*, 1–11.
8. Kathuria, N., & Seet, B.-C. (2021). 24 GHz flexible antenna for doppler radar-based human vital signs monitoring. *Sensors, 21*(11), 3737.
9. Bahramiabarghouei, H., Porter, E., Santorelli, A., Gosselin, B., Popovic, M., & Rusch, L. A. (2015). Flexible 16 antenna array for microwave breast cancer detection. *IEEE Transactions on Biomedical Engineering, 62*(10), 2516–2525.
10. Lilja, J., Pynttäri, V., Kaija, T., Mäkinen, R., Halonen, E., Sillanpää, H., & de Maagt, P. (2013). Body-worn antennas making a splash: Lifejacket-integrated antennas for global search and rescue satellite system. *IEEE Antennas and Propagation Magazine, 55*(2), 324–341.
11. Rezaeieh, S. A., Brankovic, A., Janani, A. S., Mohammed, B., Darvazehban, A., Zamani, A., & Abbosh, A. M. (2020). Wearable electromagnetic belt for steatotic liver detection using multivariate energy statistics. *IEEE Access, 8*, 201847–201860.
12. Haerinia, M., & Noghanian, S. (2019). A printed wearable dual-band antenna for wireless power transfer. *Sensors, 19*(7), 1732.
13. Alqadami, A. S. M., Stancombe, A. E., Bialkowski, K. S., & Abbosh, A. (2021). Flexible meander-line antenna array for wearable electromagnetic head imaging. *IEEE Transactions on Antennas and Propagation, 69*(7), 4206–4211.
14. Bharadwaj, R., Swaisaenyakorn, S., Parini, C. G., Batchelor, J., & Alomainy, A. (2014). Localization of wearable ultrawideband antennas for motion capture applications. *IEEE Antennas and Wireless Propagation Letters, 13*, 507–510.
15. Ashyap, A. Y., Elamin, N. I. M., Dahlan, S. H., Abidin, Z. Z., See, C. H., Majid, H. A., & Esmail, B. A. F. (2021). Via-less electromagnetic band-gap-enabled antenna based on textile material for wearable applications. *PLoS ONE, 16*(1), e0246057.
16. Ashyap, A. Y., Dahlan, S. H. B., Abidin, Z. Z., Rahim, S. K. A., Majid, H. A., Alqadami, A. S., & El Atrash, M. (2021). Fully fabric high impedance surface-enabled antenna for wearable medical applications. *IEEE Access, 9*, 6948–6960.
17. Gao, G.-P., Hu, B., Wang, S.-F., & Yang, C. (2018). Wearable circular ring slot antenna with EBG structure for wireless body area network. *IEEE Antennas and Wireless Propagation Letters, 17*(3), 434–437.
18. Yin, B., Gu, J., Feng, X., Wang, B., Yu, Y., & Ruan, W. (2019). A low sar value wearable antenna for wireless body area network based on Amc structure. *Prog. Electromagn. Res. C, 95*(April), 119–129.
19. El Atrash, M., Abdalgalil, O. F., Mahmoud, I. S., Abdalla, M. A., & Zahran, S. R. (2020). Wearable high gain low SAR antenna loaded with backed all-textile EBG for WBAN applications. *IET Microwaves, Antennas and Propagation, 14*(8), 791–799.
20. Gao, G., Wang, S., Zhang, R., Yang, C., & Hu, B. (2020). Flexible EBG-backed PIFA based on conductive textile and PDMS for wearable applications. *Microwave and Optical Technology Letters, 62*(4), 1733–1741.
21. Bait-Suwailam, M. M., Labiano, I. I., & Alomainy, A. (2020). Impedance enhancement of textile grounded loop antenna using High-Impedance Surface (HIS) for healthcare applications. *Sensors, 20*(14), 3809.
22. El Atrash, M., Abdalla, M. A., & Elhennawy, H. M. (2021). A compact flexible textile artificial magnetic conductor-based wearable monopole antenna for low specific absorption rate wrist applications. *International Journal of Microwave and Wireless Technologies, 13*(2), 119–125.
23. Pei, R., Leach, M. P., Lim, E. G., Wang, Z., Song, C., Wang, J., & Huang, Y. (2020). Wearable EBG-backed belt antenna for smart on-body applications. *IEEE Transactions on Industrial Informatics, 16*(11), 7177–7189.
24. Ashyap, A. Y., Dahlan, S. H. B., Abidin, Z. Z., Dahri, M. H., Majid, H. A., Kamarudin, M. R., & Abbasi, Q. H. (2020). Robust and efficient integrated antenna With EBG-DGS enabled wide bandwidth for wearable medical device applications. *IEEE Access, 8*, 56346–56358.
25. Joshi, R., Hussin, E. F. N. M., Soh, P. J., Jamlos, M. F., Lago, H., Al-Hadi, A. A., & Podilchak, S. K. (2020). Dual-band, dual-sense textile antenna with AMC backing for localization using GPS and WBAN/WLAN. *IEEE Access, 8*, 89468–89478.
26. Zhang, K., Vandenbosch, G. A. E., & Yan, S. (2020). A novel design approach for compact wearable antennas based on metasurfaces. *IEEE Transactions on Biomedical Circuits and Systems, 14*(4), 918–927.
27. Sanchez-Montero, R., Lopez-Espi, P. L., Alen-Cordero, C., & Martinez-Rojas, J. A. (2019). Bend and moisture effects on the performance of a U-shaped slotted wearable antenna for off-body communications in an Industrial Scientific Medical (ISM) 24 GHz band. *Sensors, 19*(8), 1804.
28. El Atrash, M., Abdalla, M. A., & Elhennawy, H. M. (2021). A compact highly efficient Π-section CRLH antenna loaded with textile AMC for wireless body area network applications. *IEEE Transactions on Antennas and Propagation, 69*(2), 648–657.
29. Ashyap, A. Y., Abidin, Z. Z., Dahlan, S. H., Majid, H. A., & Seman, F. C. (2018). A compact wearable antenna using EBG for smart-watch applications. In *2018 Asia-Pacific Microwave Conference (APMC)* (pp. 1477-1479). IEEE

30. Kiani, S., Rezaei, P., & Fakhr, M. (2021). A CPW-fed wearable antenna at ISM band for biomedical and WBAN applications. *Wireless Networks, 27*(1), 735–745.
31. De Cos Gómez, M. E. D., Berdasco, A. F., Álvarez, H. F., & Las-Heras, F. (2020). On the way to green IoT antennas: Compact ultra-thin CPW-fed monopole on tencel. In *2020 14th European Conference on Antennas and Propagation (EuCAP)* (pp. 1-5). IEEE.
32. Seman, F. C., Ramadhan, F., Ishak, N. S., Yuwono, R., Abidin, Z. Z., Dahlan, S. H., & Ashyap, A. Y. I. (2019). Performance evaluation of a star-shaped patch antenna on polyimide film under various bending conditions for wearable applications. *Progress In Electromagnetics Research Letters, 85*, 125–130.
33. Lee, H., & Choi, J. (2017). A compact all-textile on-body SIW antenna for IoT applications. In *2017 IEEE International Symposium on Antennas and Propagation & USNC/URSI National Radio Science Meeting* (pp. 825-826). IEEE
34. Trinh, L., Le, T., Staraj, R., Ferrero, F., & Lizzi, L. (2017). A pattern-reconfigurable slot antenna for IoT network concentrators. *Electronics, 6*(4), 105.
35. Sabban, A. (2019). Small new wearable antennas for IOT, medical and sport applications. In *2019 13th European Conference on Antennas and Propagation (EuCAP)* (pp. 1–5). IEEE.
36. Kumar, S., Buckley, J. L., Barton, J., Newberry, R., Dunlop, G., Rodencal, M. & O'Flynn, B. (2019). A bandwidth enhanced 915 MHz antenna for IoT wrist-watch applications. In *2019 13th European Conference on Antennas and Propagation (EuCAP)* (pp. 1-5). IEEE
37. Mustaqim, M., Khawaja, B. A., Chattha, H. T., Shafique, K., Zafar, M. J., & Jamil, M. (2019). Ultra-wideband antenna for wearable Internet of Things devices and wireless body area network applications. *International Journal of Numerical Modelling: Electronic Networks, Devices and Fields, 32*(6), e2590.
38. Ramos, A., Varum, T., & Matos, J. (2018). Compact multilayer Yagi-Uda based antenna for IoT/5G sensors. *Sensors, 18*(9), 2914.
39. Loss, C., Gonçalves, R., Lopes, C., Pinho, P., & Salvado, R. (2016). Smart coat with a fully-embedded textile antenna for IoT applications. *Sensors, 16*(6), 938.
40. de Cos Gómez, M. E., Fernández Álvarez, H., Flórez Berdasco, A., & Las-Heras Andrés, F. (2020). Paving the way to eco-friendly IoT antennas: Tencel-based ultra-thin compact monopole and its applications to ZigBee. *Sensors, 20*(13), 3658.
41. Azeez, H., Yang, H.-C., & Chen, W.-S. (2019). Wearable triband E-shaped dipole antenna with low SAR for IoT applications. *Electronics, 8*(6), 665.
42. de Cos Gómez, M. E., Fernández Álvarez, H., Puerto Valcarce, B., García González, C., Olenick, J., & Las-Heras Andrés, F. (2019). Zirconia-based ultra-thin compact flexible CPW-fed slot antenna for IoT. *Sensors, 19*(14), 3134.
43. Banerjee, S., Singh, A., Dey, S., Chattopadhyay, S., Mukherjee, S., & Saha, S. (2019). SIW based body wearable antenna for IoT applications. In *2019 International Conference on Opto-Electronics and Applied Optics (Optronix)* (pp. 1-4). IEEE
44. Byondi, F. K., & Chung, Y. (2019). Longest-range UHF RFID sensor tag antenna for IoT applied for metal and non-metal objects. *Sensors, 19*(24), 5460.
45. Nate, K., & Tentzeris, M. M. (2015). A novel 3-D printed loop antenna using flexible NinjaFlex material for wearable and IoT applications. In *2015 IEEE 24th Electrical Performance of Electronic Packaging and Systems (EPEPS)* (pp. 171-174). IEEE
46. Potey, P. M., & Tuckley, K. (2020). Design of wearable textile antenna for low back radiation. *Journal of Electromagnetic Waves and Applications, 34*(2), 235–245.

Adel Y. I. Ashyap received the B.Eng., M.Eng. and Ph.D. Degree in Electrical Engineering from Universiti Tun Hussein Onn Malaysia (UTHM), in 2012, 2014, 2019, respectively. He is currently a Postdoctoral Fellow with the Research Center of Applied Electromagnetics, Faculty of Electrical and Electronic Engineering, Universiti Tun Hussein Onn Malaysia (UTHM), Johor, Malaysia. He has authored and co-authored numbers of journals and proceedings. His research interests include electromagnetic bandgap (EBG), artificial magnetic conductor (AMC) for wireless body area networks (WBAN), microstrip antennas and small antennas for biomedical devices. He was received Chancellor Award for his final year project and a number of Gold, Silver and Bronze medals in international and local competitions.

S. H. Dahlan received his Ph.D. degree in Signal Processing and Telecommunications from the Universite de Rennes 1, France, in 2012. He is a Senior Lecturer with the Faculty of Electric and Electronic Engineering, Universiti Tun Hussein Onn Malaysia (UTHM) since March 2012. Currently he is with the Research Center for Applied Electromagnetics (EMCenter, UTHM) as the principal researcher and appointed as the Head of the center since April 2015. He has authored and co-authored numbers of journals including the IEEE Transaction on Electromagnetic Compatibility and IEEE AWPL. His research interest includes Optical-Microwave generator, focusing system (dielectric lens and transmitarray's synthesis), computational electromagnetic technique namely the BOR-FDTD and material characterizations. He is supervising a numbers of Ph.D, master's, and bachelor's students and involved in several research projects sponsored by the industry and government agencies.

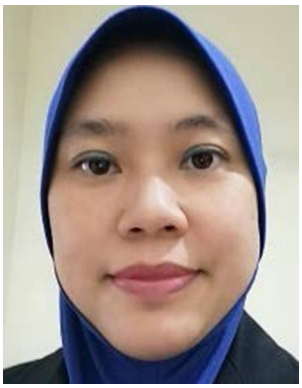

Z. Z. Abidin the Ph.D. degree from Bradford University, U.K., in 2011.Currently, she is a Head of Advanced Telecommunication Research Center (ATRC), Faculty of Electrical and Electronic Engineering, Universiti Tun Hussein Onn Malaysia. She has authored and co-authored numbers of journals and proceedings. Her research interests include MIMO antenna, printed microstrip antenna, wearable antennas, metamaterial resonator, electromagnetic bandgap (EBG) for wireless and mobile, and high-speed digital circuit's applications.

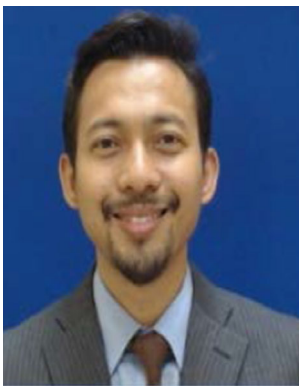

M. R. Kamarudin (M'08 - SM'13) received the degree (Hons.) majoring in Electrical and Telecommunication Engineering from Universiti Teknologi Malaysia, Johor Bahru, Malaysia, in 2003, and the M.Sc. degree in Communication Engineering and the Ph.D. degree in Electrical Engineering from the University of Birmingham, Birmingham, U.K., in 2004 and 2007, respectively, under the supervision of Emeritus Professor Peter Hall. He has been an Associate Professor with the Faculty of Electrical and Electronic Engineering, Universiti Tun Hussein Onn Malaysia since May 2019. Prior to this appointment, he was a Senior Lecturer with the Centre for Electronic Warfare, Information and Cyber, Cranfield Defense and Security, Cranfield University, U.K., and an Associate Professor with the Wireless Communication Centre, Universiti Teknologi Malaysia. He holds a SCOPUS H-Index of 23 with over 2000 citations. He has authored a book chapter of a book entitled Antennas and Propagation for Body-Centric Wireless Communications and has published over 240 technical papers in leading journals and international proceedings including the IEEE Transaction on Antennas and Propagation, the IEEE Antennas and Wireless Propagation Letter, the IEEE Antenna Magazine, the IEEE Access, the International Journal of Antennas and Propagation, Progress in Electromagnetic Research, Microwave and Optical Technology Letters, and Electronics Letters. His research interests include antenna design for 5G/6G, MIMO antennas, Array antenna for beam-forming and beam steering, wireless on-body communications, in-body communications (implantable antenna), RF and microwave communication systems, and antenna diversity. He is a Member of IET, an Executive Member of Antenna and Propagation, Malaysia Chapter, and a Member of the IEEE Antennas and Propagation Society, the IEEE Communication Society, the IEEE Microwave Theory and Techniques Society, the IEEE Electromagnetic Compatibility Society, an Associate Editor for Electronics Letters and IET Microwaves, Antennas and Propagation, and an Academic Editor for the International Journal of Antennas and Propagation.

H. A. Majid received the B Eng. degree in Electrical Engineering (Telecommunication) from Universiti Teknologi Malaysia, in 2007. He then obtained his M.Eng in 2010 and PhD degrees in Electrical Engineering in 2013, at Universiti Teknologi Malaysia. He is currently a lecturer in the Department of Electrical Engineering Technology, Faculty of Engineering Technology, Universiti Tun Hussein Onn Malaysia. His research interest includes the areas of design of microstrip antennas, small antennas, Reconfigurable antennas, metamaterials structure, metalaterial antennas and millimeter wave antennas. He has published over 50 articles in journals and conference papers.

Nayef Abdulwahab Mohammed Alduais received the B.Eng. degree in Computer Engineering from Hodeidah University,Yemen, in 2007, and the Master and Ph.D. degree in Communication and Computer Engineering from Faculty of Electrical and Electronic Engineering(FKEE), Universiti Tun Hussein Onn Malaysia (UTHM), Malaysia, in 2015 and 2019, respectively. He is currently a Lecturer and researcher in the Internet of Things (IoT) at Faculty of Computer Science and Information Technology (FSKTM), UTHM, having previously worked as an Assistant Lecturer with the Faculty of Computer Science and Engineering, Hodeidah University, Yemen, from 2007 to 2013. He has authored numerous papers in journals and conference proceedings. His research interests include WSN and IoT. He received numerous medals and scientific excellence certificates.

M. Hashim Dahri received the B.E degree in Telecommunications from the Mehran University of Engineering and Technology (MUET), Pakistan, in 2010, the Masters by Research degree in Electrical Engineering from Universiti Tun Hussein Onn Malaysia (UTHM) in 2014 and the Ph.D degree from the Wireless Communication Centre (WCC), Univerisiti Teknologi Malaysia (UTM) in 2019. After compliton of his Ph.D he worked as a postdoc research fellow in Universiti Tun Hussein Onn Malaysia (UTHM) for one year. He is currently working as an assistant Professor in the department of electronic engineering, Dawood University of Engineering and Technology Karachi, Pakistan. He has authored over 40 research papers in various indexed journals and conference proceedings. His research interests include reflectarray

antennas, planar printed antennas and tunable materials for antenna design.

Somya Abdulkarim Alhandi received the B.E degree in Computer Science (Software Engineering) with the First Class Honours. She is currently working as a Research Assistant with the Faculty of Computer Science and Information Technology, Universiti Tun Hussein Onn Malaysia. Her research interests include IoT, WSN, Trust Evaluation Model, and Trustworthy.